A Novel Approach to Analyze Membrane Proteins by Laser Mass Spectrometry: From Protein Subunits to the Integral Complex

Nina Morgner,[a] Thomas Kleinschroth,[b] Hans-Dieter Barth,[a] Bernd Ludwig,[b,c] and Bernhard Brutschy[a]

[a] Institute for Physical and Theoretical Chemistry, Johann Wolfgang Goethe University, Frankfurt am Main, Germany
[b] Molecular Genetics Group, Institute of Biochemistry, Johann Wolfgang Goethe University, Frankfurt am Main, Germany
[c] Centre of Excellence "Macromolecular Complexes," Johann Wolfgang Goethe University, Frankfurt am Main, Germany

A novel laser-based mass spectrometry method termed LILBID (laser-induced liquid bead ion desorption) is applied to analyze large integral membrane protein complexes and their subunits. In this method the ions are IR-laser desorbed from aqueous microdroplets containing the hydrophobic protein complexes solubilized by detergent. The method is highly sensitive, very efficient in sample handling, relatively tolerant to various buffers, and detects the ions in narrow, mainly low-charge state distributions. The crucial experimental parameter determining whether the integral complex or its subunits are observed is the laser intensity: At very low intensity level corresponding to an ultrasoft desorption, the intact complexes, together with few detergent molecules, are transferred into vacuum. Under these conditions the oligomerization state of the complex (i.e., its quaternary structure) may be analyzed. At higher laser intensity, complexes are thermolyzed into subunits, with any residual detergent being stripped off to yield the true mass of the polypeptides. The model complexes studied are derived from the respiratory chain of the soil bacterium *Paracoccus denitrificans* and include complexes III (cytochrome bc_1 complex) and IV (cytochrome *c* oxidase). These are well characterized multi-subunit membrane proteins, with the individual hydrophobic subunits being composed of up to 12 transmembrane helices. (J Am Soc Mass Spectrom 2007, 18, 1429–1438) © 2007 American Society for Mass Spectrometry

Biological membranes enclose and compartmentalize cells of all organisms, acting as effective insulators and selective filters between the cytoplasm and the outside medium. Being composed mainly of a double layer of phospholipids, each membrane houses a particular set of proteins or protein complexes, allowing for specific communication between the inside of a cell and its environment. Membrane proteins are centrally involved in basic cellular activities such as solute and ion transport, energy transduction in respiratory and photosynthetic systems, sensory stimuli transduction and information processing; thus they are important drug targets. Although around 20–30% of all genes are estimated to encode membrane proteins [1], our understanding for this important class of proteins lags behind for reasons of their highly hydrophobic nature, their intricate subunit structure, and their elaborate and, in many cases, only transient interaction with soluble or other membrane-bound proteins.

Both their individual polypeptide composition and their specific assembly into larger protein complexes (i.e., their quaternary structure in the membrane) are fundamental aspects in the molecular description of their functionality. Because of their insolubility in aqueous media the analysis of membrane proteins is notoriously difficult. Physicochemical studies of membrane proteins generally require detergent treatment for solubilization, and many studies have focused on protein–detergent interactions from both functional and structural perspectives.

Since the late 1980s, mass spectrometry (MS) has increasingly been applied to the studies of proteins because of its high mass accuracy, allowing one to identify even small posttranslational modifications. The mass analysis of noncovalent protein complexes is another, still challenging goal of mass spectrometry. Presently, mainly electrospray ionization (ESI)–MS [2] and matrix-assisted laser desorption/ionization (MALDI)–MS [3], often coupled to high-performance liquid chromatography (HPLC), are used. ESI-MS has

Address reprint requests to Prof. B. Brutschy, Institute for Physical and Theoretical Chemistry, J.W. Goethe University, Max-von-Lavestr 9, 60438 Frankfurt, Germany. E-mail: brutschy@chemic.uni-frankfurt.de.

1044-0305/07/$32.00
doi:10.1016/j.jasms.2007.04.013

Published online April 29, 2007
Received March 2, 2007
Revised April 20, 2007
Accepted April 24, 2007

developed from a method to determine the molecular mass of single proteins into a tool for studying noncovalent multimeric protein assemblies ([4–6] and references cited within). In particular the ESI-MS analysis of several important soluble macromolecular complexes has been reported [7, 8]. However, the study of detergent-solubilized proteins with ESI-MS is demanding because of protein signal suppression resulting from the presence of excess detergent [9, 10]. Thus analysis by ESI-MS usually requires the removal of detergent by organic solvents before sample analysis [11–15].

Whereas ESI-MS is now extensively used for the study of noncovalent complexes, the application of MALDI-MS in this area of research is more restricted. Nevertheless MALDI was used to analyze water-soluble proteins with molecular weights up to 300 kDa [16] and MALDI data on the subunit stoichiometry of high mass noncovalent complexes of membrane proteins have been reported by van Dorsselaer et al. [17] and Gennis et al. [18].

Compared with these established MS methods, experiments with laser-induced liquid bead ion desorption (LILBID)–MS [19], pioneered by our group [20–23], are relatively straightforward in handling.

The biomolecules, dissolved in aqueous, buffered solution, are laser desorbed/ablated from microdroplets (average diameter 50 μm, volume 65 pL) into vacuum. For desorption the wavelength of the IR laser is tuned to the absorption maximum of water at around 3 μm, corresponding to an excitation of the stretching vibrations of water. At a threshold intensity of around 100 MW/cm^2 a very fast phase transition is induced concomitant with a spherical explosion and subsequent disruption of the droplet. This results in the emission of ions from liquid into gas phase, where they can be mass analyzed by time-of-flight (TOF) spectrometry. From as low as one single droplet to, more typically, only 100 to 200 droplets are sufficient to record a mass spectrum, depending on the analyte concentration.

In the following we show that, at very low laser intensity, LILBID works in a very gentle way, which allows detection of intact membrane complexes [i.e., the complete assembly of all subunits (ultrasoft mode)]. At intermediate laser intensities (semisoft mode), complexes are partially thermolyzed into subcomplexes and subunits. Finally, at still higher intensities, the hydrophobic interactions are broken up completely and only the individual subunits are observed in the mass spectrum (harsh mode).

Thus our approach to study the membrane molecules is "top-down" and not "bottom-up," as is typical in methods used in modern proteomics.

In a proof of principle experiment, we focus on components of the respiratory chain of the soil bacterium *Paracoccus denitrificans*. It has been extensively studied as a model organism of the mitochondrial electron-transfer chain for its simple subunit composition, yet full functionality and its high sequence identity [24]. Apart from other energy-converting branches, the core part of the respiratory chain system in *P. denitrificans* is highly homologous to its mitochondrial counterpart, and consists of four complexes: NADH:ubiquinone oxidoreductase (complex I); succinate:ubiquinone oxidoreductase (complex II); ubiquinol:cytochrome *c* oxidoreductase (bc_1 complex, complex III); and cytochrome *c* oxidase (aa_3 oxidase, complex IV), linked by the two-electron carrier ubiquinone and the one-electron carrier cytochrome *c*. Here we specifically analyze complexes III and IV, as well as cytochrome *c*, which in the case of *P. denitrificans* is the membrane-bound cytochrome c_{552}. These proteins and complexes were chosen because (i) their subunit masses are known from primary sequence, (ii) they allow a wide variation in the degree of complexity in terms of subunit composition and number of transmembrane helices (TMH) present in each subunit, and (iii) the three-dimensional (3-D) structures of complex IV and of the heme domain of cytochrome c_{552} have already been solved [25, 26].

Experimental

Measurement of LILBID Spectra

In the older version of the LILBID technique, based on continuous liquid beams, which are still applied presently [27, 28], a large consumption of analyte excluded application to the mass analysis of biomolecules of low availability. The new version, however, now uses liquid droplets [19], which minimizes the analyte consumption by orders of magnitude. The microdroplets (ϕ = 50 μm) are produced on demand by a piezo-driven droplet generator and introduced by differential pumping stages into the vacuum, where they are irradiated one by one by intense nanosecond mid-IR laser pulses. The laser pulses are generated in a home-built optical parametric oscillator (OPO) based on a $LiNbO_3$ crystal pumped by a commercial pulsed Nd-Yag laser. The moderately focused laser pulses (spot size around 300 μm in diameter, pulse duration around 6 ns) are tuned to a wavelength of about λ = 3 μm, at pulse energies of 1 to 15 mJ/pulse, depending on the amount of desired fragmentation.

At this wavelength centered in the broad absorption band of liquid water, the laser energy is absorbed by the O—H stretch vibrations of the water molecules within the first micrometers of the liquid surface of the droplet. At a threshold intensity of around 100 MW/cm^2 a very fast phase transition is induced concomitant with a spherical explosion and subsequent disruption of the droplet resulting in the emission of ions from liquid into gas phase. These ions are then accelerated in a conventional pulsed two-field ion optic and mass analyzed in a home-built TOF reflectron mass spectrometer [19]. To detect very large biomolecular ions with high *m/z* values we use a home-built Daly-type ion detector, working up to an *m/z* range in the low megadalton region. For the present study only anions were ana-

Table 1. Properties of three soluble *c*-type cytochromes analyzed by LILBID-MS

Cytochrome	Isoelectric point	Charge at pH 7[a]	LILBID anion charge states[b]	Mass (kDa)	LILBID mass (kDa)
Horse heart cyt *c*	10.0–10.5	9.2	0	12.4	12.3
Cyt c_1 CF	4.2	–22.2	4	23.4	23.9
Cyt c_{552} fragment	5.3	–3.7	1	10.5	10.9

[a]Number of charge states as calculated from their amino acid sequence.
[b]Number of charge states as observed in LILBID-MS.

lyzed, corresponding to the net charge states of most of these proteins in solution. However, cation spectra may also be obtained, although in the case of biomolecules in general at much lower intensity.

Especially under ultrasoft desorption conditions the mass spectra often exhibit, apart from discrete ion peaks, a broad unstructured ion background, caused by metastable loss of water and buffer molecules. In those cases the broad background was subtracted from the original ion spectra. To improve the signal-to-noise ratio these difference spectra were smoothed by averaging the signal over a preset number of channels of the transient recorder, with the smoothing interval always lying within the time resolution of our TOF mass spectrometer. The spectra were mass calibrated with proteins of known mass such as lysozyme (14.3 kDa), bovine serum albumin (67 kDa), catalase (60 kDa as monomer and 240 kDa as a tetramer), and with DNA strands of different lengths, recorded under identical conditions of the apparatus.

Sample Preparation

For the initial solubilization of the membrane proteins and for all further purification steps the nonionic detergent *n*-dodecyl-β-D-maltoside (DDM; mass = 511 Da), which maintains in vitro enzymatic activity (see reference cited below) was used, if not specified otherwise. For all LILBID experiments reported here, we used ammonium acetate as standard buffer, in general at a concentration of 25 mM, and at pH 6.8 containing 0.025% (wt/vol) of DDM. For typical measurements only 2–10 μL of sample solution is required, containing the analyte in micromolar concentration. The amount of protein present in one single droplet is typically in the femto- to attomole region. Under typical conditions the recorded mass spectra are averages over 100 to 200 laser shots and droplets, respectively.

Preparation of cytochrome c_{552}. Heterologous expression of the His-tagged full-length cytochrome c_{552} and its solubilization and purification were performed as described by Drosou et al. [29]. The final buffer used in the LILBID experiments was introduced by ultrafiltration (Vivaspin, 10-kDa cutoff).

Cytochrome bc_1 complex. The wild-type *P. denitrificans* bc_1 complex was purified from a strain overexpressing the protein; cell growth, membrane isolation, solubilization, and subsequent protein purification were done essentially as described in Schröter et al. [30], with modifications described in Ritter et al. [31]. For buffer exchange, ultrafiltration (Vivaspin 100-kDa cutoff) was used.

Cytochrome c oxidase. To obtain the four-subunit preparation [26], the protein was purified from wild-type membranes solubilized in DDM as described in Hendler et al. [32]. A two-subunit enzyme complex was purified in Triton X-100 according to Ludwig and Schatz [33]; in a final purification step this detergent was exchanged for DDM by DEAE anion-exchange chromatography followed by ultrafiltration (Vivaspin 100-kDa cutoff).

Cytochrome c_{552} fragment. This soluble module of 100 amino acids, prepared as described by Reincke et al. [34] (see Table 1), constitutes the heme-binding domain, but lacks the N-terminal membrane anchor; its 3-D structure is known [25].

Cytochrome c_1 CF. This soluble, acidic fragment of 220 amino acids (see Table 1) represents the heme-binding domain and was expressed in *E. coli* (Janzon et al., unpublished observations).

Mixture of the Three Soluble Cytochromes

Equimolar amounts (at a concentration of 100 μM each, determined spectroscopically) of three soluble cytochromes (horse heart cytochrome *c*, the c_{552} fragment and the c_1 CF fragment; see above) were combined and the mixture was dialyzed extensively (4-kDa cutoff membrane) against 50 mM ammonium acetate buffer at pH 6.8 and then diluted 10-fold for MS measurements.

Chemicals

n-Dodecyl-β-D-maltoside (DDM) was obtained from Merck (Darmstadt, Germany), 2-(*N*-morpholino)ethanesulfonic acid (MES) buffer was from AppliChem (Darmstadt, Germany), ammonium acetate (buffer grade) was from Roth (Karlsruhe, Germany), and horse heart cytochrome *c* was from Sigma–Aldrich (Deisenhofen, Germany). All aqueous solutions were made with deionized water.

Calibration Standards

Hen egg lysozyme and catalase were purchased from Sigma–Aldrich, bovine serum albumin from Biomol (Hamburg, Germany), and single-stranded DNA of defined length from Biospring (Frankfurt, Germany).

The proteins were dissolved in water and DNA strands in 10 mM ammonium acetate at pH 7.

Results and Discussion

Ion Formation Mechanism and Mass Resolution

Although the ion formation process for LILBID is still not well characterized, we favor a "lucky survivor" model for its rationalization [21]. In this model the photon absorption induces a very fast nonequilibrium phase transition beyond the supercritical point, from where the liquid expands explosively similar to an ideal highly compressed gas [19]. In the decreasing particle density of the rapidly expanding supercritical phase, the dielectric constant drops to zero [35], and the no-longer-shielded ions and counter ions start to recombine. Only those ions escape into vacuum that are too far away from their counter ions to be trapped by Coulomb attraction [36]. About one and 10,000 of the solvated ions in the liquid thus escape into vacuum. Thus preformed ions are detected as the result of an incomplete ion neutralization process.

Because of the spherical isotropic explosive expansion (with a velocity of around 800 m/s) of the ion cloud, the present resolving power is limited in the kilodalton mass range to an approximated $M/\Delta M$ value of 100, and a value even lower in mass ranges above. This limitation in mass resolution, which cannot be compensated by the delayed field technique, may eventually be overcome by collisional cooling in an ion trap and a pulsed storage depletion with subsequent orthogonal acceleration of the ions for TOF analysis, which is presently under development in our laboratory.

Residual Detergent

Any mass analysis of a complex membrane protein by MS faces two major challenges: (i) the efficient transfer of the ionic species into vacuum and (ii) a careful appraisal of the fate of the detergent molecules used to solubilize the protein. Detergents are amphipathic molecules, mimicking the native lipid bilayer environment of the isolated protein under investigation. The hydrophobic surface areas of the latter are covered by the apolar hydrocarbon chains of the detergent molecules such as dodecyl maltoside, forming either a micellar structure or a monolayer around the protein, preventing its nonspecific aggregation in aqueous solution [37]. DDM (m/z = 511) has proved to be a very useful detergent for studying a large number of membrane proteins, by providing excellent properties for solubilization and purification in monodisperse form and in preserving the enzymatic activity at the same time [38, 39].

Quantitative studies showed that the number of bound detergent molecules correlates with the size of the hydrophobic surface exhibited by a complex. Typical numbers of DDM molecules bound to membrane complexes similar in size to those studied here range between 150 and 200 [37]. It should be noted that any detergent micelle surviving the desorption process would shift the observed mass of the detected ion to considerably higher masses, easily discriminated by MS. To investigate the fate of such DDM micelles during the LILBID desorption process, we started out with the bacterial cytochrome c_{552} as a simple prototypic membrane protein, consisting of only a single transmembrane helix (TMH) in its hydrophobic part.

This cytochrome shuttles electrons between the bc_1 complex and cytochrome *c* oxidase in *P. denitrificans*. Its TMH is located N-terminally and is connected by a linker region to the hydrophilic C-terminus of the protein liganding the heme cofactor. For purification purposes, it was expressed heterologously with an additional hexa-His tag at its extreme N-terminus, yielding a calculated mass of around 20 kDa (see Table 2) for the polypeptide, making any mass shift arising from attached detergent molecules readily detectable within the mass resolution of our spectrometer.

Figure 1 depicts the mass spectrum of this single polypeptide. The prominent mass peaks correspond to the molecular ions M^- (m/z = 19,700) and M^{2-} (m/z = 9900). By comparing this value to the calculated mass it is obvious that neither the whole detergent micelle nor even any single detergent molecule has survived the desorption process. Even under greatly differing desorption conditions, that is, with harsh and soft conditions applied by varying the laser intensity (see also below), no detergent contribution was observable.

Two minor, closely spaced double peaks observed in the spectrum spectrum, one pair at 14,600 and 14,800 m/z and another at 5000 and 5200 m/z, are neither fragment ions produced by the laser desorption process, nor any impurities, but represent proteolysis products generated at nearby sites of the polar part of the protein, which were not separated in the chromatographic preparation of the sample before mass analysis. This assignment is supported by the fact that the two ion masses add up to the expected full-size protein mass. In addition, the larger species corresponds to a fragment recognized by specific anti-cytochrome c_{552} antibodies in a Western blot analysis (not shown).

Next we addressed the question of whether the complete loss of all detergent molecules similarly holds true for membrane proteins exhibiting a more complex topology of TMHs, characterized by grooves between adjacent TMHs, that may favor a stronger binding of detergent molecules.

Table 2. Subunit composition and masses of the detected ions of selected respiratory membrane protein complexes

Protein	Subunit (SU)	Number of TMHs	Number of AAs	Isoelectric point	Charge at pH 7[a]	LILBID anion charge states[b]	Apparent mass (kDa)[c]	Mass (kDa)[d]	LILBID mass (kDa)[e]
Cytochrome c_{552}		1	184	5.5	–9.0	2	26	19.9	19.7
Complex III	ISP	1	190	4.3	–9.5	1	20	20.4	20.1
Complex III	cytc_1	1	426	3.8	–76.0	3	60	45.3	45.0
Complex III	cyt*b*	8	440	6.2	–4.7	1	40	51.4	49.6
Complex IV	SU I	12	558	6.4	–4.4	2	45	64.1	62.3
Complex IV	SU II	2	252	4.6	–11.6	2	28	28.1	27.9
Complex IV	SU III	7	273	6.0	–5.0	2	23	30.6	30.6
Complex IV	SU IV	1	49	6.6	–0.5	1	5	5.4	5.4

[a]Number of charges in solution as calculated from their amino acid sequence.
[b]Number of charge states as observed in LILBID-MS.
[c]Apparent molecular mass deduced from SDS-PAGE (for details, see reference cited in the text).
[d]Deduced from sequence.
[e]Molecular mass derived from LILBID-MS.

Complex IV: Cytochrome c Oxidase

Cytochrome *c* oxidase, also termed complex IV, is a structurally far more elaborate membrane protein. It oxidizes cytochrome c_{552} and transfers electrons to the terminal acceptor of the respiratory chain, dioxygen, with the free energy of this reaction coupled to transmembrane proton translocation [40,41]. The structure of complex IV from *P. denitrificans* is known with high resolution [26]. This enzyme is composed of four hydrophobic subunits of different complexities (see Table 2 for details). Subunit I consists of 12 transmembrane helices and is almost completely buried in the membrane with only short connecting loops. It carries three redox centers (two hemes *a* and the copper B center [26]). Subunit II has a split architecture with the two membrane-spanning α-helices in its N-terminal domain and a 10-stranded β-barrel hydrophilic domain at the C-terminus, which houses the Cu_A center. The seven helices of subunit III are highly hydrophobic and completely embedded in the membrane, lacking any redox centers, whereas subunit IV consists of essentially a single TMH [42]. A functionally active version of this complex may also be isolated that lacks subunits III and IV [33].

A mass spectrum of the solubilized complex IV, taken under very mild desorption conditions, is given in Figure 2a. The oxidase complex appears as a regular sequence of broad mass peaks, corresponding to different charge states of the complex, ranging from one to five negative charges. Because the mass of the detected complex is >126 kDa (see below), apparently no major fragmentation into individual subunits occurs under these conditions.

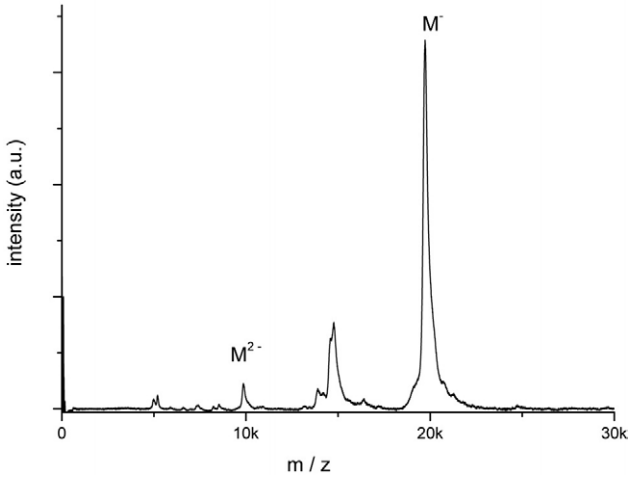

Figure 1. LILBID mass spectrum of cytochrome c_{552}. The molecule peak (M) is observed singly and doubly charged. At 5000 and 5200 *m/z* and at 14,600 and 14,800 *m/z* two proteolytic fragments not separated by the previous purification steps are visible (see text).

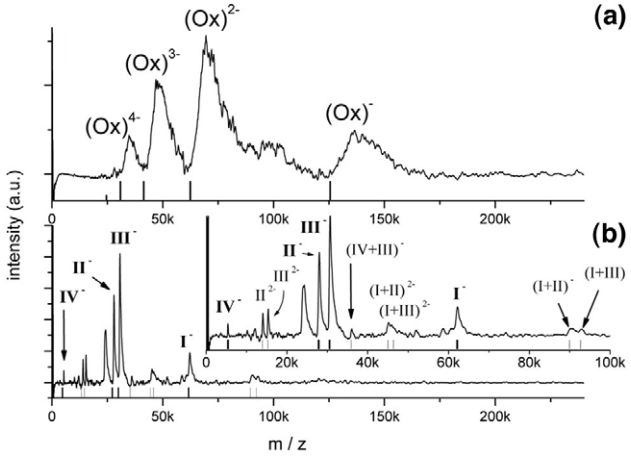

Figure 2. Mass spectra of the four-subunit cytochrome *c* oxidase complex. (**a**) The anion spectrum taken under ultrasoft desorption conditions. The intact oxidase complex is visible; the black stick spectrum below the experimental trace indicates the theoretical mass/charge ratio for oxidase ions with charges between 1 and 4. The band broadening is attributed to residual detergent molecules and/or water still adhering to the complex (see text). (**b**) The same spectrum measured under harsh desorption conditions. The theoretical positions of the four subunits are indicated by a stick spectrum (black). Further ion signals are assigned to subcomplexes and doubly charged molecules (gray lines; see text). A peak at 24,000 *m/z* could not be accounted for.

It should be noted that the center of the mass peaks is shifted to *m/z* values larger than the theoretical ones of oxidase, indicated at the bottom of the trace by a stick spectrum. In addition, the shape of the mass peaks is not quite symmetric, with a rising edge a little steeper compared to the more slowly falling edge trailing to higher masses. Because such broad peaks are observed only under ultrasoft desorption conditions, this peak shape may be rationalized mostly by residual detergent molecules still attached to the molecular ion of the complex. We cannot exclude the possibility that residual phospholipids and water molecules adhere as well.

This contrasts with the situation of a protein carrying only a single TMH such as the cytochrome c_{552} discussed earlier, where the surrounding micelle did not survive the ion desorption process. With proteins of more complex transmembrane secondary structure such as oxidase, however, some of the detergent molecules together with water molecules obviously remain attached, broadening and shifting the mass peaks toward higher *m/z* values. It appears plausible that detergent molecules buried in the grooves between helices, especially, are bound more firmly and therefore survive the ionization process. The onset of the mass peaks is located at the theoretical values. If one assumes that the peak broadening is preferentially caused by residual detergent molecules, the position of the peak maxima (corresponding to a molecular weight of 132 kDa with $z = 1$ to 4) suggests that an average of 20 to 25 molecules of DDM survive the desorption. According to the estimated number of initially bound detergent molecules (see above), this would correspond to about 10–15% of the initial detergent molecules that remain attached to the protein complex. Considering the distribution of the oxidase signals corresponding to a molecular weight of 126 kDa ($z = 1$ to 4) plus detergents, it is obvious that the four-subunit oxidase is present as a monomer under the conditions of the present study, which confirms earlier findings [43, 44].

To disintegrate the complex into its subunits for analyzing their mass, the intensity of the desorption laser has to be increased stepwise. With additional energy transferred into the complex by elevated laser power, noncovalent interactions between the subunits are broken up, releasing the four oxidase subunits for MS analysis as separate macromolecules. Figure 2b depicts the mass spectrum under such conditions, where all four subunits (I–IV) are observed singly charged. However, subunits II and III show higher intensities and also appear as doubly charged ions. These differences between subunits with identical stoichiometry in the complex may be rationalized by the higher net charge of subunits II and III at neutral pH in solution. The response function of the LILBID process obviously favors the detection of ions according to their net charge state in solution, as will be discussed more thoroughly in the context of the findings for bc_1 complex.

In addition ion signals of minor intensity can be observed in the spectrum, as can be seen more clearly in

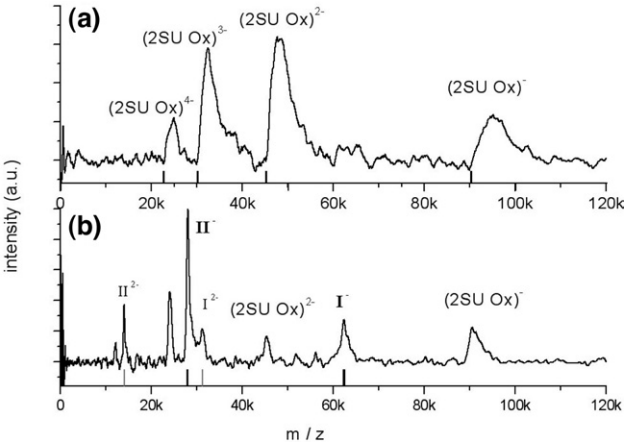

Figure 3. Mass spectrum of the two-subunit (2SU) cytochrome *c* oxidase. (**a**) under ultrasoft desorption conditions: The intact complex appears at four different charge states (black stick spectrum indicates the theoretical mass/charge positions) (**b**) measured with higher laser power. The intensity of the intact complex decreases and ion signals of the individual subunits show up (indicated by black stick spectrum; doubly charged ions indicated by gray stick spectrum). The subunit ions lack any additional detergent molecules and the remaining complex peaks reveal that the residual detergents have been further diminished. The peak at 24,000 *m/z* remains unexplained; if it represents an impurity from the purification procedure, it is not resolved in the standard SDS gel control.

the enlarged part of Figure 2b. They are assignable to subcomplexes composed of heterodimers of subunits such as I + II, I + III, and III + IV. It should be pointed out that no dimers II + III, II + IV, or homodimers are observed. The detectable subcomplexes consist of adjacent subunits and obviously arise from an incomplete fragmentation of the native complex. Thus the intensity and composition of these subcomplexes reflect the next-neighbor relationships of subunits, optimized for their contact areas and thus for stronger hydrophobic interactions in the complex. These conclusions are in very good agreement with the structure of the oxidase complex as determined by X-ray diffraction [26]. Thus random aggregation of subunits by gas-phase reactions can clearly be excluded.

A modified cytochrome *c* oxidase complex containing only subunits I and II was also investigated for comparison. This fully functional oxidase complex results from a purification procedure using Triton X-100 ([33]; and see above), effectively removing subunits III and IV. Under the most gentle desorption conditions this complex appears as several charge states, ranging from one to four negative charges (Figure 3a). Again the mass peaks of the complex are substantially broadened and shifted to higher masses, mainly as the result of residual detergent and possibly water molecules. For the two-subunit oxidase it has been shown that all phospholipids are removed by this stringent purification process [33]. So the maximum of the detergent-based peak broadening corresponds to 10–12 residual DDM molecules, indicating a relative loss of detergent

molecules (based on the number of respective THMs) comparable to that of the four-subunit oxidase.

Upon increasing the laser power, the ion signals of the intact complex decrease and those of the two individual subunits I and II dominated the spectrum, as shown in Figure 3b. Under these harsher conditions no major contributions of detergent molecules are observed for the subunit ions, and for the reduced signal of the intact complex a strongly diminished residual detergent contribution is seen.

Complex III: Cytochrome bc_1 Complex

Another multisubunit membrane protein of the bacterial respiratory chain, which we analyzed by LILBID-MS is the cytochrome bc_1 complex, also known as complex III. The structure of this protein isolated from different mitochondrial sources such as yeast is known from X-ray diffraction (e.g., [45]). Complex III transfers electrons from ubiquinol to cytochrome *c*. During this reaction protons are translocated across the membrane by the Q-cycle, contributing to the generation of the proton gradient. The bacterial complex analyzed here consists of three subunits: (i) the Rieske iron–sulfur protein (ISP), which has an N-terminal TMH and an extensive C-terminal hydrophilic domain connected through a flexible linker region; (ii) the cytochrome *b*, which is highly hydrophobic (see Table 2) with its eight TMHs almost completely buried in the membrane, binding the two *b* heme cofactors noncovalently; and (iii) cytochrome c_1 with a C-terminal transmembrane anchor and a *c*-type heme cofactor [46]. Several lines of evidence indicate at least a dimeric structure both for the mitochondrial and the bacterial complex III. Crystal structures for both types (e.g., [45, 47, 48]) show a mutually intertwined organization for the ISP subunit, being embedded in one monomer by its N-terminal anchor, while serving the other monomer in a mechanism described as a major movement of the FeS cofactor domain during intracomplex electron transfer [49]. Dimeric [44] and even higher oligomeric structures have been observed by other techniques as well, such as gel filtration and blue native PAGE [50].

Under "gentle" desorption conditions, the intact complex is also detected here as well. As depicted in Figure 4a, the mass spectrum shows a series of peaks that clearly correspond to a charge distribution of the bc_1 complex, oligomerized to a tetramer. To distinguish between the ion distribution of a multiply charged dimer and tetramer, the corresponding stick spectra are included schematically in Figure 4b and c. The experimental spectrum gives no indication for the presence of a dimer, nor any other unspecific oligomeric forms. This indicates that the tetramer is probably the native quaternary structure of the complex in solution as well as in a supercomplex stoichiometry. Referring to the intertwined structure of the two monomers, it should rather be regarded as a pair of dimers. Again the mass peaks of the integral complex are considerably broadened as a result of residual detergent and/or water molecules surviving the desorption process. However, it should be pointed out that the overall detergent-induced broadening of the mass peaks of the bc_1 complex differs from that of cytochrome *c* oxidase.

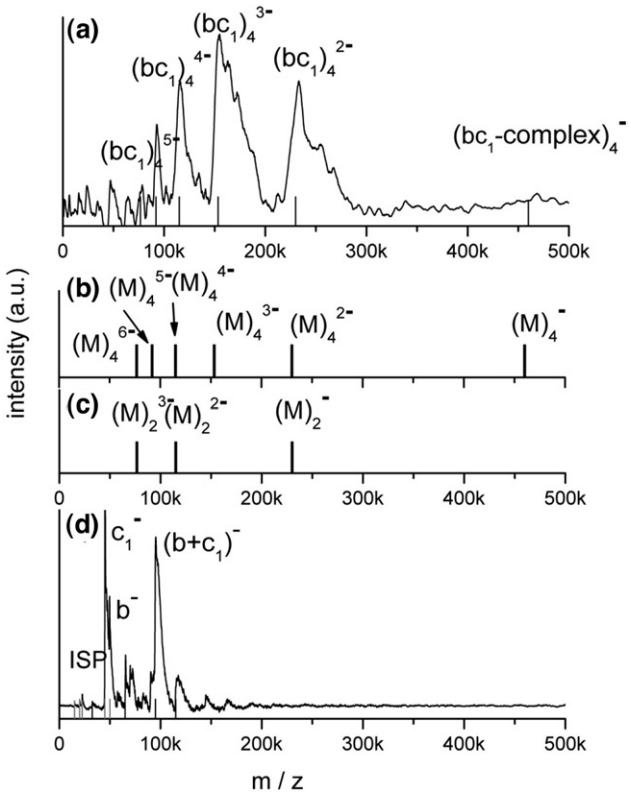

Figure 4. Mass spectrum of the cytochrome bc_1 complex. (**a**) At low laser intensity the bc_1 complex is detected as a tetramer, as deduced by comparison with the theoretical charge distributions for the bc_1-complex, calculated in (**b**) for a tetramer and (**c**) for a dimer. (**d**) Upon increase of the laser intensity the complex desintegrates into subcomplexes and the individual subunits. Further details are depicted in Figure 6.

For the bc_1 complex the peak maxima correspond to the theoretical mass/charge values of the tetrameric bc_1 complex with only very few residual detergent molecules attached, and a detergent distribution directly trailing off toward larger numbers of residual detergents. The peak shapes for the oxidase ions on the other hand are different (see Figure 2a), with their observed maxima shifted by a mass increase corresponding to 20 to 25 additional DDM molecules.

A possible explanation for the different numbers of residual detergent molecules in case of the four-/two-subunit oxidase and the tetrameric bc_1 complex, respectively, may be found in a different ruggedness of the hydrophobic landscape, leading to a different affinity for binding and, thus, for retaining detergent molecules resulting from the laser desorption.

Figure 4d shows a spectrum of the same sample when analyzed at elevated laser intensity (20 mJ/pulse). The intact tetrameric complex is no longer visible because of the enhanced thermal energy input

into the liquid droplets. Consequently, only individual subcomplexes and subunits appear in the lower mass region of the spectrum.

Because the interaction between the cytochrome *b* and the cytochrome c_1 subunits is stronger than that between the cytochrome c_1 and the Rieske protein (mainly embedded in the other monomer; see above), the $(b + c_1)$ subcomplexes survive with higher probability than the (Rieske + c_1) subcomplexes at desorption conditions, which are already too harsh for the integral tetramer to withstand. Therefore, similar to the case of oxidase, next-neighbor relationships of proteins in the complex are qualitatively reflected in the mass spectra (Figure 5a). Upon further increase of the laser power (Figure 5b) these binary subcomplexes are dissociated as well.

Although cytochrome *b* and the Rieske subunit are observed in the spectrum only as singly charged species, the ion signal of the cytochrome c_1 polypeptide is very intense and in addition appears in the higher charge states. These different ion intensities and charge states of subunits that are present in equimolar amounts in the complex, correlate in some way with the net charge of the ions in solution, as calculated from their amino acid sequence (see Table 2). The most intense mass peak in Figure 6 based that of the cytochrome c_1 subunit, which in addition is present in the three different charge states. The cytochrome *b* and the Rieske protein, on the other hand, carry only a single charge and both appear at strongly reduced intensities in the LILBID mass spectrum. A clear correlation between the charge state in solution and in the gas phase is evident.

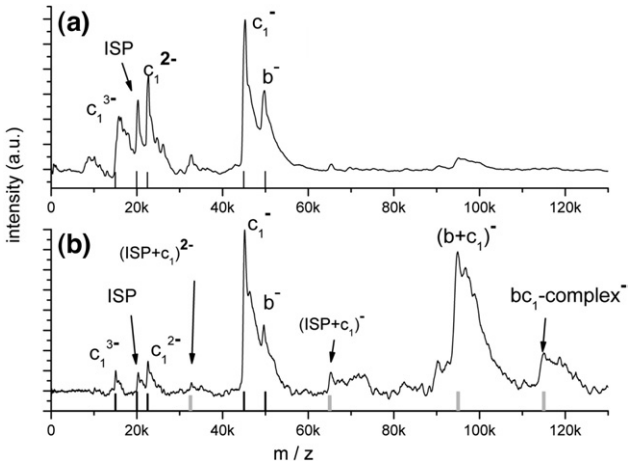

Figure 5. Mass spectra of the cytochrome bc_1 complex at elevated laser intensity (**a**) at very harsh desorption conditions only the subunits survive (indicated by black sticks), (**b**) at more gentle conditions also subcomplexes (gray sticks) of the subunits appear, yielding information on their binding contacts with adjacent subunits in the complex.

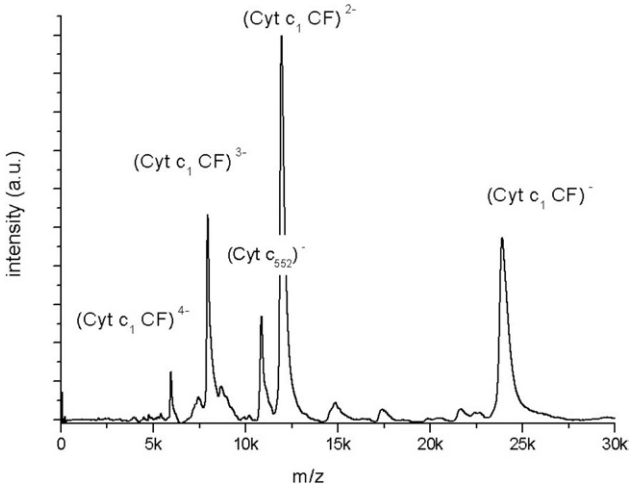

Figure 6. Mass spectrum of an equimolar mixture of three different soluble cytochromes *c*, differing in their isoelectric points. Cytochrome c_1 CF with the lowest IP shows the most intense signals and a charge distribution from 1 to 4. The cytochrome c_{552} fragment, with an intermediate isoelectric point, is less intense and appears only singly charged, whereas horse heart cytochrome *c* with its strong positive net charge cannot be seen.

Charge Distribution of the Proteins in Gas Phase in View of Their Isoelectric Point

To further verify this correlation between the charge state of proteins in solution and their ion signal in the mass spectrum three different soluble cytochromes *c* were investigated, chosen both for their different isoelectric points (see Table 1) and therefore different net charges at neutral pH (Figure 6), and for their simple spectroscopic quantitation by their heme groups. MS spectra were recorded at neutral pH in the standard buffer (omitting the detergent) at equimolar concentration for each of the cytochromes.

As expected, cytochrome c_1 CF (isoelectric point: 4.2) yields the most intensive peaks with a negative charge distribution from 1 to 4. Less intense is the signal of cytochrome c_{552}, which appears only singly charged. The horse heart cytochrome *c* with an isoelectric point > 10 is not visible in the anion spectrum at all. In the combined cytochrome solution MS assay it might be difficult to resolve because its mass is close to the doubly charged cytochrome c_1 CF, although measurements of horse heart cytochrome *c* alone confirmed the negative result (not shown).

These data support the "lucky survivor" mechanism suggested for LILBID: Because it postulates an incomplete ion neutralization in the explosive expansion of the preformed ions, one expects the molecules with higher charge state in aqueous solution to have a larger neutralization-escape probability than the less charged species, purely for statistical reasons. So a higher endogenous charge on a polypeptide results in a larger ion recovery and a distribution of higher charge states of the ion peaks.

By these arguments different charge distributions of the ions in a LILBID measurements qualitatively reflect

the net charge present in solution as derived from their amino acid sequence (Table 2).

From the present still scarce data it is too early to discuss the charge state question quantitatively and in greater depth. What we report here are trends, which are differently pronounced for the different proteins. This may be because ion recombination should also be dependent on the site of the charge, the local dielectric constant, ion strength, and so forth. At least the comparison of, for example, the subunits cytochrome $c_{1\delta}$ and cytochrome *b* from complex III (Figure 5), which are of similar mass but with very different charge state and peak intensity, clearly shows that the average charge per mass is not comparable. This speaks against a mass/size-dependent statistical charged distribution.

Along this line of argument clearly, because of the charge-dependent LILBID response function for proteins, the relative peak intensities and the mass spectrum cannot be used to determine intrinsic stoichiometries of subunits in a given complex or in a protein mixture.

Conclusions

LILBID-MS is a very promising method for the soft mass analysis of membrane proteins because it allows the transfer of large macromolecular complexes into the gas phase of the mass spectrometer. Simply by varying the level of laser intensity in the desorption process, different stages of the disintegration of the membrane protein complex can be achieved. At low-energy conditions even very large integral complexes are transferred into vacuum and may be detected unfragmented, revealing their oligomeric association state. Depending on the complexity of the hydrophobic part of the proteins up to 15% of the detergent molecules remain bound to the macromolecule under these ultrasoft conditions. At elevated laser intensity, however, these residual detergent molecules are stripped off concomitant with the complex disintegrating into its subcomplexes and eventually into its protein subunits. The response function of this mass spectrometry favors the detection of the more highly charged proteins in solution, and their appearance at higher charged states in the gas-phase LILBID mass spectrum, thus reflecting tendencies of solution behavior.

Because it requires only very small sample quantities (in the picomole range) with solution volumes in the microliter range LILBID–MS opens new avenues for the mass spectrometry of complex membrane proteins. Its relative tolerance toward detergents is a crucial advantage over other MS methods. It is as soft as a non-denaturating gel but it has at least one order of magnitude higher mass accuracy compared to that of electrophoretic analysis, where the determined masses of polypeptides may be put off by excessive hydrophobicity or charge. Moreover, the mass analysis of even highly hydrophobic subunits, which are difficult to analyze by conventional MS methods, is easily amenable by use of this technique. Further advantages in comparison to analytical ultracentrifugation [51] are the facts that LILBID requires no complicated experimental determination of the amount of bound detergent and needs only very small amounts of analyte. The still modest mass resolution, obtained with our home-built TOF, can readily be improved by coupling the LILBID ion source to a high-resolution mass spectrometer. For a future setup the additional option to sequence the subunit proteins by multidimensional MS (MS^n) is currently being developed.

Acknowledgments

The authors thank Werner Müller for excellent technical assistance and Julia Janzon for providing the cytochrome c_1 fragment. The authors also acknowledge financial support from Collaborative Research Centers Grants SFB 472 and 579.

References

1. Heijne, G. v. Membrane-Protein Topology. *Nat. Rev. Mol. Cell. Biol.* **2006**, *7*, 909–918.
2. Fenn, J. B.; Mann, M.; Meng, C. K.; Wong, S. F.; Whitehouse, C. M. Electrospray Ionization for Mass Spectrometry of Large Biomolecules. *Science* **1989**, *246*, 64–71.
3. Tanaka, K.; Waki, H.; Ido, Y.; Akita, S.; Yoshida, Y.; Yoshida, T. Protein and Polymer Analyses up to *m/z* 100 000 by Laser Ionization Time-of-Flight Mass Spectrometry. *Rapid Commun. Mass Spectrom.* **1988**, *2*, 151–153.
4. Sobott, F.; Robinson, C. V. Protein Complexes Gain Momentum. *Curr. Opin. Struct. Biol.* **2002**, *12*, 729–734.
5. Miranker, A. D. Protein Complexes and Analysis of Their Assembly by Mass Spectrometry. *Curr. Opin. Struct. Biol.* **2000**, *10*, 601–606.
6. Loo, J. A. Studying Noncovalent Protein Complexes by Electrospray Ionization Mass Spectrometry. *Mass Spectrom. Rev.* **1997**, *16*, 1–23.
7. Rostom, A. A.; Fucini, P.; Benjamin, D. R.; Juenemann, R.; Nierhaus, K. H.; Hartl, F. U.; Dobson, C. M.; Robinson, C. V. Detection and Selective Dissociation of Intact Ribosomes in a Mass Spectrometer. *Proc. Natl. Acad. Sci. U.S.A.* **2000**, *97*, 5185–5190.
8. Fitzgerald, M. C.; Chernushevich, I.; Standing, K. G.; Whitman, C. P.; Kent, S. B. Probing the Oligomeric Structure of an Enzyme by Electrospray Ionization Time-of-Flight Mass Spectrometry. *Proc. Natl. Acad. Sci. U.S.A.* **1996**, *93*, 6851–6856.
9. Loo, R. R. O.; Dales, N.; Andrews, P. C. Surfactant Effects on Protein -Structure Examined by Electrospray-Ionization Mass-Spectrometry. *Protein Sci.* **1994**, *3*, 1975.
10. Rundlett, K. L.; Armstrong, D. W. Mechanism of Signal Suppression by an Ionic Surfactant in Capillary Electrophoresis Electrospray Ionization Mass Spectrometry. *Anal. Chem.* **1996**, *68*, 3493–3497.
11. Whitelegge, J. P.; Gomez, S. M.; Faull, K. F. Proteomics of Membrane Proteins. *Adv. Protein Chem.* **2003**, *65*, 271–307.
12. Whitelegge, J. P. Tandem Mass Spectrometry of Integral Membrane Proteins for Top-down Proteomics. *TrAC, Trends Anal. Chem.* **2005**, *24*, 576–582.
13. Whitelegge, J. P.; Le Coutre, J.; Lee, J. C.; Engel, C. K.; Privè, G. G.; Faull, K. F.; Kaback, H. R. Toward the Bilayer Proteome, Electrospray Ionization-Mass Spectrometry of Large, Intact Transmembrane Proteins. *Proc. Natl. Acad. Sci. U.S.A.* **1999**, *96*, 10695–10698.
14. Hufnagel, P.; Schweiger, U.; Eckerskorn, C.; Oesterhelt, D. Electrospray Ionization Mass Spectrometry of Genetically and Chemically Modified Bacteriorhodopsins. *Anal. Biochem.* **1996**, *243*, 46–54.
15. Caroll, J.; Fearnley, I. M.; Walker, J. E. Definition of the Mitochondrial Proteome by Measurements of Molecular Masses of Membrane Proteins. *Proc. Natl. Acad. Sci. U.S.A.* **2006**, *103*, 16170–16175.
16. Cohen, S. L.; Chait, B. T. Mass Spectrometry of Whole Proteins Eluted from Sodium Dodecyl Sulfate–Polyacrylamide Gel Electrophoresis Gels. *Anal. Biochem.* **1997**, *247*, 257–267.
17. Schindler, P. A.; Van Dorsselaer, A.; Falick, A. M. Analysis of Hydrophobic Proteins and Peptides by Electrospray Ionization Mass Spectrometry. *Anal. Biochem.* **1993**, *213*, 256–263.
18. Ghaim, J. B.; Tsatsos, P. H.; Katsonouri, A.; Mitchell, D. M.; Salcedo-Hernandez, R.; Gennis, R. B. Matrix-Assisted Laser Desorption Ionization Mass Spectrometry of Membrane Proteins: Demonstration of a Simple Method to Determine Subunit Molecular Weights of Hydrophobic Subunits. *Biochim. Biophys. Acta* **1997**, *1330*, 113–120.
19. Morgner, N.; Barth, H.-D.; Brutschy, B. A New Way to Detect Noncovalently Bonded Complexes of Biomolecules from Liquid Micro-Droplets by Laser Mass Spectrometry. *Aust. J. Chem.* **2006**, *59*, 109–114.
20. Sobott, F.; Schunk, S. A.; Schüth, F.; Brutschy, B. Examination of Condensation Products of Group 4 Alkoxides with Laser-Induced

Liquid Beam Ionization/Desorption Mass Spectrometry. *Chem. Eur. J.* **1998**, *4*, 2353–2359.
21. Kleinekofort, W.; Avdiev, J.; Brutschy, B. A New Method of Laser Desorption Mass Spectrometry for the Study of Biological Macromolecules. *Int. J. Mass Spectrom. Ion Processes* **1996**, *152*, 135–142.
22. Kleinekofort, W.; Pfenninger, A.; Plomer, T.; Griesinger, C.; Brutschy, B. Observation of Noncovalent Complexes Using Laser-induced Liquid Beam Ionization/Desorption. *Int. J. Mass Spectrom. Ion Processes* **1996**, *156*, 195–202.
23. Kleinekofort, W.; Schweitzer, M.; Engels, J.; Brutschy, B. Analysis of Double-stranded Oligonucleotides by Laser-induced Liquid Beam Mass Spectrometry. *Int. J. Mass Spectrom. Ion Processes* **1997**, *163*, L1–L4.
24. Baker, S. C.; Ferguson, S. J.; Ludwig, B.; Page, M. D.; Richter, O.-M. H.; van Spanning, R. J. M. Molecular Genetics of the Genus *Paracoccus*—Metabolically Versatile Bacteria with Bioenergetic Flexibility. *Microbiol. Mol. Biol. Rev.* **1998**, *62*, 1046–1078.
25. Harrenga, A.; Reincke, B.; Rüterjans, H.; Ludwig, B.; Michel, H. Structure of the Soluble Domain of Cytochrome c_{552} from *Paracoccus denitrificans* in the Oxidized and Reduced States. *J. Mol. Biol.* **2000**, *295*, 667–678.
26. Iwata, S.; Ostermeier, C.; Ludwig, B.; Michel, H. Structure at 2.8 Å Resolution of Cytochrome *c* Oxidase from *Paracoccus denitrificans*. *Nature* **1995**, *376*, 660–669.
27. Charvat, A.; Bogehold, A.; Abel, B. Time-resolved Micro Liquid Desorption Mass Spectrometry: Mechanism, Features, and Kinetic Applications. *Aust. J. Chem.* **2006**, *59*, 81–103.
28. Kohno, J. Y.; Toyama, N.; Buntine, M. A.; Mafune, F.; Kondow, T. Gas Phase Ion Formation from a Liquid Beam of Arginine in Aqueous Solution by IR Multiphoton Excitation. *Chem. Phys. Lett.* **2006**, *420*, 18–23.
29. Drosou, V.; Reincke, B.; Schneider, M.; Ludwig, B. Specificity of Interaction between the *Paracoccus denitrificans* Oxidase and Its Substrate Cytochrome *c*: Comparing the Mitochondrial to the Homologous Bacterial Cytochrome c_{552}, and Its Truncated and Site-directed Mutants. *Biochemistry* **2002**, *41*, 10629–10634.
30. Schröter, T.; Hatzfeld, O. M.; Gemeinhardt, S.; Korn, M.; Friedrich, T.; Ludwig, B.; Link, T. A. Mutational Analysis of Residues Forming Hydrogen Bonds in the Rieske [2Fe2S] Cluster of the Cytochrome bc_1 Complex in *Paracoccus denitrificans*. *Eur. J. Biochem.* **1998**, *255*, 100–106.
31. Ritter, M.; Anderka, O.; Ludwig, B.; Mäntele, W.; Hellwig, P. Electrochemical and FTIR Spectroscopic Characterization of the bc_1 Complex from *Paracoccus denitrificans*: Evidence for Protonation Reactions Coupled with Quinone Binding. *Biochemistry* **2003**, *42*, 12391–12399.
32. Hendler, R. W.; Pardhasaradhi, K.; Reynafarje, B.; Ludwig, B. Comparison of Energy-transducing Capabilities of the Two- and Three-Subunit Cytochromes aa_3 from *Paracoccus denitrificans* and the 13-Subunit Beef Heart Enzyme. *Biophys. J.* **1991**, *60*, 415–423.
33. Ludwig, B.; Schatz, G. A Two-Subunit Cytochrome mdit>c Oxidase (Cytochrome aa_3) from *Paracoccus denitrificans*. *Proc. Natl. Acad. Sci. U.S.A.* **1980**, *77*, 196–200.
34. Reincke, B.; Thöny-Meyer, L.; Dannehl, C.; Odenwald, A.; Aidim, M.; Witt, H.; Rüterjans, H.; Ludwig, B. Heterologous Expression of Soluble Fragments of Cytochrome c_{552} Acting as Electron Donor to the *Paracoccus denitrificans* Cytochrome *c* Oxidase. *Biochim. Biophys. Acta* **1999**, *1411*, 114–120.
35. Franck, E. U.; Deul, R. Dielectric Behaviour of Methanol and Related Polar Fluids at High Pressures and Temperatures. *Faraday Discuss. Chem. Soc.* **1978**, *66*, 191–198.
36. Dessiaterik, Y.; Nguyen, T.; Baer, T.; Miller, R. E. IR Vaporization Mass Spectrometry of Aerosol Particles with Ionic Solutions: The Problem of Ion–Ion Recombination. *J. Phys. Chem. A* **2003**, *107*, 11245–11252.
37. Moller, J. V.; le Maire, M. Detergent Binding as a Measure of Hydrophobic Surface Area of Integral Membrane Proteins. *J. Biol. Chem.* **1993**, *268*, 18659–18672.
38. Seddon, A. M.; Curnow, P.; Booth, P. J. Membrane Proteins, Lipids and Detergents: Not Just Soap Opera. *Biochim. Biophys. Acta* **2004**, *1666*, 105–117.
39. Garavito, R. M.; Ferguson-Miller, S. Detergents as Tool in Membrane Biochemistry. *J. Biol. Chem.* **2001**, *276*, 32403–32406.
40. Richter, O.-M. H.; Ludwig, B. Cytochrome *c* Oxidase—Structure, Function, and Physiology of a Redox-driven Molecular Machine. *Rev. Physiol. Biochem. Pharmacol.* **2003**, *147*, 47–74.
41. Hosler, J. P.; Ferguson-Miller, S.; Mills, D. A. Energy Transduction: Proton Transfer through the Respiratory Complexes. *Annu. Rev. Biochem.* **2006**, *75*, 165–187.
42. Witt, H.; Ludwig, B. Isolation, Analysis, and Deletion of the Gene Coding for Subunit IV of Cytochrome *c* Oxidase in *Paracoccus denitrificans*. *J. Biol. Chem.* **1997**, *272*, 5514–5517.
43. Ludwig, B.; Grabo, M.; Gregor, I.; Lustig, A.; Regenass, M.; Rosenbusch, J. Solubilized Cytochrome *c* Oxidase from *Paracoccus denitrificans* is a Monomer. *J. Biol. Chem.* **1982**, *257*, 5576–5578.
44. Mayer, G.; Anderka, O.; Ludwig, B.; Schubert, D. The State of Association of the bc_1 Complex from *Paracoccus denitrificans* in Solutions of Dedecyl Maltoside. *Prog. Colloid Polym. Sci.* **2002**, *119*, 77–83.
45. Hunte, C.; Koepke, J.; Lange, C.; Rossmanith, T.; Michel, H. Structure at 2.3 Å Resolution of the Cytochrome bc_1 Complex from the Yeast *Saccharomyces cerevisiae* Co-crystallized with an Antibody Fv-Fragment. *Structure* **2000**, *8*, 669–684.
46. Kurowski, B.; Ludwig, B. The Genes of the *Paracoccus denitrificans* bc_1 Complex—Nucleotide Sequence and Homologies between Bacterial and Mitochondrial Subunits. *J. Biol. Chem.* **1987**, *262*, 13805–13811.
47. Elberry, M.; Xiao, K.; Esser, L.; Xia, D.; Yu, L.; Yu, C. A. Generation, Characterization and Crystallization of a Highly Active and Stable Cytochrome bc_1 Complex Mutant from *Rhodobacter sphaeroides*. *Biochim. Biophys. Acta* **2006**, *1757*, 835–840.
48. Berry, E. A.; Huang, L.-S.; Saechao, L. K.; Pon, N. G.; Valkova-Valchanova, M.; Daldal, F. X-ray Structure of *Rhodobacter capsulatus* Cytochrome bc_1: Comparison with Its Mitochondrial and Chloroplast Counterparts. *Photosynth. Res.* **2004**, *81*, 251–275.
49. Berry, E. A.; Guergova-Kuras, M.; Huang, L.-S.; Crofts, A. R. Structure and Function of Cytochrome *bc* Complexes. *Annu. Rev. Biochem.* **2000**, *69*, 1005–1075.
50. Stroh, A.; Anderka, O.; Pfeiffer, K.; Yagi, T.; Finel, M.; Ludwig, B.; Schägger, H. Assembly of Respiratory Complexes I, III, and IV into NADH Oxidase Supercomplex Stabilizes Complex I in *Paracoccus denitrificans*. *J. Biol. Chem.* **2004**, *279*, 5000–5007.
51. Howlett, G. J.; Minton, A. P.; Rivas, G. Analytical Ultracentrifugation for the Study of Protein Association and Assembly. *Sci. Direct* **2006**, *10*, 430–436.